

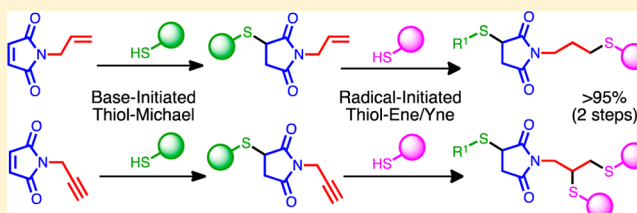
Experimental and Theoretical Studies of Selective Thiol–Ene and Thiol–Yne Click Reactions Involving *N*-Substituted Maleimides

Robert M. Stolz and Brian H. Northrop*

Department of Chemistry, Wesleyan University, Middletown, Connecticut 06459, United States

S Supporting Information

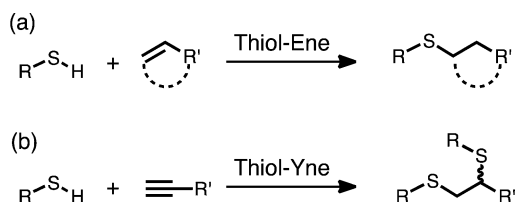
ABSTRACT: A combination of experimental and computational methods has been used to understand the reactivity and selectivity of orthogonal thiol–ene and thiol–yne “click” reactions involving *N*-allyl maleimide (**1**) and *N*-propargyl maleimide (**2**). Representative thiols methyl-3-mercaptopropionate and β -mercaptoethanol are shown to add exclusively and quantitatively to the electron poor maleimide alkene of **1** and **2** under base (Et_3N) initiated thiol–Michael conditions. Subsequent radical-mediated thiol–ene or thiol–yne reactions can be carried out to further functionalize the remaining allyl or propargyl moieties in near quantitative yields (>95%). Selectivity, however, can only be achieved when base-initiated thiol–Michael reactions are carried out first, as radical-mediated reactions between equimolar amounts of thiol and *N*-substituted maleimides give complex mixtures of products. CBS–QB3 calculations have been used to investigate the energetics and kinetics of reactions between a representative thiol (methyl mercaptan) with *N*-allyl and *N*-propargyl maleimide under both base-initiated and radical-mediated conditions. Calculations help elucidate the factors that underlie the selective base-initiated and nonselective radical-mediated thiol–ene/yne reactions. The results provide additional insights into how to design selective radical-mediated thiol–ene/yne reactions.



■ INTRODUCTION

Advances in thiol–ene chemistry¹ have been rapid over the past ten years, as the highly versatile reactivity of thiols with alkenes (Scheme 1a) has been utilized across multiple areas of

Scheme 1. General Representations of Thiol–Ene (a) and Thiol–Yne (b) “Click” Chemistries



macromolecular,² biomolecular,³ and materials chemistry.⁴ Even more recently, the reactivity of thiols with alkynes⁵ (Scheme 1b) has gained similar prominence in areas of polymers and soft materials. Both reactions, thiol–ene and thiol–yne, can be carried out under a variety of reaction conditions and in the presence of a range of functional groups, displaying many of the hallmarks of so-called click^{6–8} chemistry. Thiol–ene chemistry can be carried out using radical initiators,^{2c} basic or nucleophilic initiators,⁹ and under solvent-promoted conditions¹⁰ to give thioethers in high to quantitative yields. Thiol–yne reactions are typically radical-mediated processes, giving 1,2-diaddition products with similar yields.⁵ As the utility and versatility of both thiol–ene and thiol–yne chemistry have become increasingly apparent there

has been significant interest in achieving selective, orthogonal thiol–ene and thiol–yne click reactions.

In 2009, Chan et al. reported the first example of sequential thiol–ene/thiol–yne reactions.¹¹ In their study a phosphine initiator was used to promote the Michael addition of a thiol exclusively to the acrylate double bond of propargyl acrylate. This thiol–Michael reaction was directly followed by radical-mediated addition of the same or a different thiol to the alkyne moiety. This sequential, orthogonal thiol–click process has since been used to prepare a variety of macromolecular materials such as selectively end-functionalized *N*-isopropylacrylamide homopolymers,¹² multifunctional dendrimers,¹³ and “two-stage” polymer networks¹⁴ with applications in optical materials, shape memory polymers, and imprint lithography.

We report herein experimental and theoretical investigations aimed at elucidating the underlying details of selective, orthogonal thiol–ene and thiol–yne reactions. *N*-Substituted maleimides¹⁵ are used in base initiated thiol–Michael reactions, while allyl and propargyl functionalities allow for subsequent radical-mediated thiol–ene and thiol–yne chemistry, respectively. Selectivity, however, is only achieved when the thiol–Michael reaction is performed first – i.e. carrying out radical-mediated thiol–click reactions first leads to a mixture of addition products. This sensitivity to the order of reaction conditions follows what has been shown^{9,11} previously in sequential thiol–ene/thiol–yne reactions. Computational investigations of the

Received: July 3, 2013

Published: July 31, 2013

relative energetics of anionic and radical-mediated thiol–ene and thiol–yne reactions are able to aid in explaining this experimentally observed selective reactivity under thiol–Michael conditions and nonselective reactivity under radical-mediated conditions. The combination of experimental and theoretical results provides a significantly enhanced understanding of the energetic and kinetic factors that underlie the selectivity and efficiency of anionic and radical-mediated thiol–ene reactions. The theoretical framework described can be used to help design the first example(s) of selective radical-mediated thiol–ene reactions in complex ternary mixtures, opening the door to more facile syntheses of complex macromolecular materials.

RESULTS AND DISCUSSION

Thiol–Michael reactions can be initiated by amines or phosphines^{9,11} that are able to react through deprotonation of a thiol, nucleophilic addition to the π -bond of an alkene, or a combination of both. The specific mechanism is influenced by the pK_a of the thiol and nature of the alkene as well as the pK_a and sterics of the base/nucleophile. Both Chan et al.^{9a} and Li et al.^{9b} have evaluated the ability of different basic and nucleophilic reagents to initiate thiol–Michael reactions and found that trisubstituted phosphines, particularly tri-*n*-propylphosphine and dimethylphenylphosphine, provide the fastest overall reactivity. The amount of phosphine initiator should be kept low, however, as their nucleophilic addition into alkene π -systems is known to produce undesired phosphamichael adducts. The formation of such side products is typically of little concern as phosphines reliably and rapidly initiate thiol–Michael reactions even when present at very low levels. Et₃N, by contrast, cleanly initiates thiol–Michael additions with no side products^{9b} but requires longer reaction times. In all cases thiol–Michael reactions are most efficient with electron deficient alkenes, and *N*-substituted maleimides have been shown^{9a} to react fastest in thiol–Michael reactions on account of its two electron-withdrawing groups and the release of ring strain upon addition.¹⁶ Radical-mediated thiol–ene reactions, by contrast, are fastest when electron rich alkenes are employed.^{1,17,18}

Thiol–Michael additions to alkynes can also be carried out under basic, nucleophilic, or transition-metal-catalysis.^{5c} Such additions, however, are only favorable for aryl and electron-poor acetylenes, e.g. ethynyl ketones, phenylacetylene, propiolic acid derivatives. Furthermore, thiolate additions to electron-deficient alkynes give vinyl sulfides rather than the 1,2-diaddition products of radical-mediated thiol–yne click chemistry. Given the differences in reactivity between electron-poor and electron-rich π -bonds toward base-initiated and radical-mediated thiol additions we prepared *N*-allyl maleimide (1) and *N*-propargyl maleimide (2) (Figure 1) as model compounds for selective thiol–ene/thiol–ene and thiol–ene/thiol–yne click reactions, respectively.

Selective Thiol–Ene/Thiol–Ene and Thiol–Ene/Thiol–Yne Reactivity. *N*-Allyl maleimide (1) was prepared according to literature procedures¹⁹ in 3 steps and 86% overall yield.

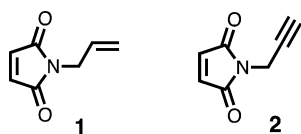


Figure 1. Structures of *N*-allyl maleimide (1) and *N*-propargyl maleimide (2).

Maleimide 1 was reacted with an equimolar amount of methyl-3-mercaptopropionate (3) in CDCl₃ in the presence of 0.01 equiv of Et₃N.²⁰ Quantitative thiol–Michael addition of 3 to the maleimide double bond of 1 was observed by NMR spectroscopy within <5 min as indicated by the complete disappearance of the maleimide singlet at 6.73 ppm (H_a), the retention of allyl signals (H_{b,d}), and the appearance of an enantiomeric doublet of doublets at 3.74 ppm (H_e) in the resulting ¹H NMR spectrum (Figure 2). The solvent, thioester

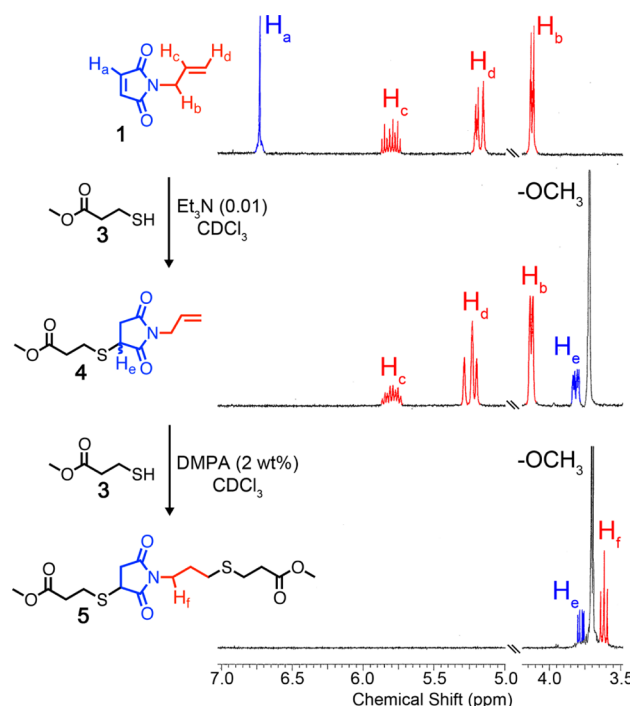
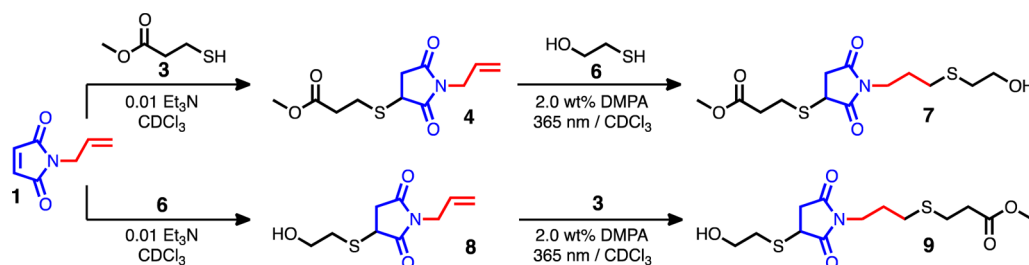


Figure 2. Partial ¹H NMR spectra (CDCl₃, 300 MHz, 298 K) of *N*-allyl maleimide (1), selective formation of 4 via base-initiated addition of thiol 3, and subsequent formation of 5 via radical-mediated addition of 3 to the allyl moiety of 4.

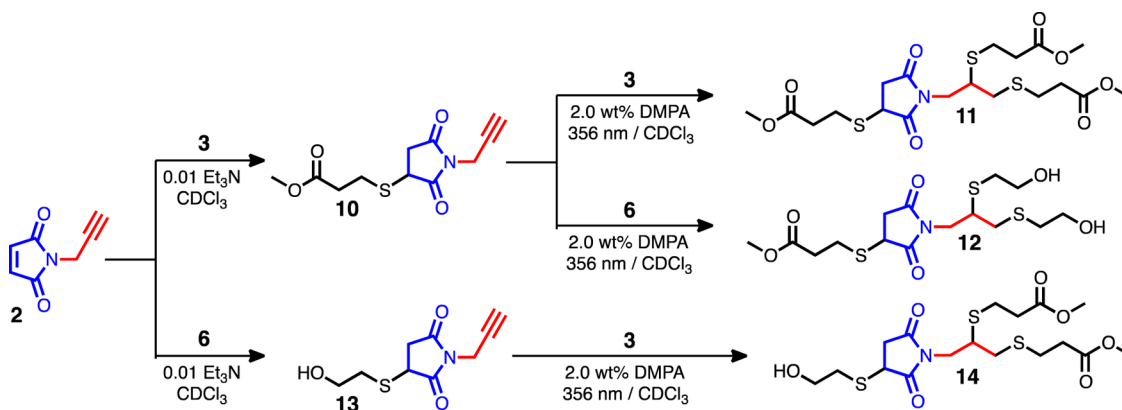
3, and Et₃N are of sufficient volatility that analytically pure thiol–Michael product 4 can be obtained following simple evaporation of the reaction mixture and drying under vacuum. In an attempt to force thiol–ene addition to the allyl moiety of 4 the compound was taken up in CDCl₃ and allowed to react with excess thiol 3 in the presence of excess Et₃N. No Et₃N-catalyzed reaction between 3 and 4 could be observed upon standing for >10 days, further demonstrating the absolute selectivity of thiolate addition to the maleimide π -bond.

The allyl functionality of 4 was subsequently reacted with an additional equivalent of 3 under radical-mediated conditions by irradiating with 365 nm light (15 W) in the presence of 2.0 wt % catalytic radical initiator α,α -dimethoxy- α -phenylacetophenone (DMPA) to give diaddition product 5 (Figure 2). Quantitative consumption of the allyl moiety of 4 was observed by ¹H NMR spectroscopy within 1 h. Alternatively, a different thiol can be reacted with the allyl functionality to achieve the completely selective, orthogonal reactivity of two different thiols with *N*-allyl maleimide 1. As a representative example, β -mercaptoethanol (6) was reacted with the allyl functionality of 4 under radical-mediated conditions to give 7 (Scheme 2). It should be noted that product 9, a structural isomer of 7, can also be synthesized by the sequential addition of 6 to 1 under thiol–Michael conditions followed directly by the radical-

Scheme 2. Synthesis of Isomeric Thiol–Ene Products 7 and 9 via the Addition of Two Different thiols (3 and 6) to *N*-Allyl Maleimide 1 by Sequential, Orthogonal Base-Initiated and Radical-Mediated Conditions



Scheme 3. Selective Base-Initiated Synthesis of Thiol–Ene Products 10 and 13 Followed by Subsequent Radical-Mediated Thiol–Yne Synthesis of Products 11, 12, and 14



mediated addition of 3. Both isomers, 7 and 9, are obtained analytically pure in >95% isolated yield over two steps without requiring laborious chromatographic purification.²¹

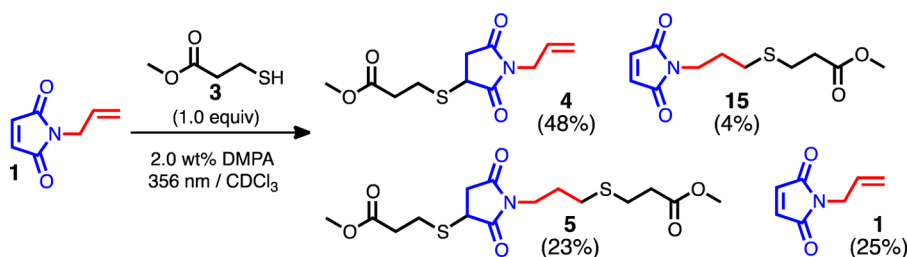
Selective, orthogonal thiol–ene/thiol–yne reactivity can also be easily achieved when starting from *N*-propargyl maleimide (2). Et₃N-initiated addition of methyl-3-mercaptopropionate (3) to *N*-propargyl maleimide (2) occurs exclusively at the maleimide alkene, giving 10 in quantitative yield within <5 min (Scheme 3). No addition of thiol 3 to the propargyl functionality was observed under thiol–Michael conditions (see Figure S1 of the Supporting Information). Following isolation of intermediate 10, 1,2-diaddition of 3 across the propargyl triple bond was carried out by irradiation at 365 nm in the presence of 2.0 wt % DMPA. Again the two-step process gives triaddition product 11 in >95% overall yield (see Table S1 of the Supporting Information) with complete selectivity while requiring no laborious purification.²¹ Selective and sequential addition of two different thiols to the maleimide and propargyl π -bonds of 2 can also be easily achieved (Scheme 3). Diol 12 was prepared by radical-mediated thiol–yne click addition of β -mercaptoethanol 6 to the propargyl moiety of 10. Likewise the Et₃N-initiated addition of 6 to *N*-propargyl maleimide (2) gives yne-ol 13 exclusively. 1,2-Diaddition of 3 to 13 under radical-mediated thiol–yne conditions gave clean conversion to product 14. It is important to reiterate that, because thiol–yne click chemistry is a 1,2-diaddition process, materials with greater overall functionality can be prepared in fewer steps using *N*-propargyl maleimide than *N*-allyl maleimide. Products arising from the sequential addition of three thiols to *N*-propargyl maleimide (2) along the route outlined in Scheme 4 will inevitably contain at least two stereocenters as neither Et₃N-initiated thiol–Michael nor radical-mediated thiol–yne reactions proceed stereospecifically. The generation of multiple

stereocenters, however, is not expected to influence the overall physical, mechanical, or thermal properties of thiol–yne-based macromolecular materials.

The use of maleimides in selective thiol–ene and thiol–yne syntheses is particularly beneficial. The fast, facile, and selective reactivity of maleimides with thiols has made thiol–maleimide reactions one of the most commonly utilized tools for bioconjugation²² of small molecules with proteins, enzymes, peptides, etc. for decades. The development of new maleimide-based selective and orthogonal means of thiol–ene/thiol–ene and thiol–ene/thiol–yne reactions can be expected to have impacts not only in the synthesis of macromolecules and new materials synthesis but also in bioorganic and biomaterials chemistries. *N*-Substituted maleimides 1 and 2 can be easily conjugated to thiol functionalities of, for example, peptides giving bioconjugates with accessible ene or yne groups that can then be further functionalized through thiol–ene or thiol–yne reactions. In this regard thiol–ene and thiol–yne chemistries may provide additional advantages to copper-catalyzed alkyne–azide (CuAAC) bioconjugation techniques²³ as they avoid the use of metal catalysts²⁴ that can be toxic to cells.

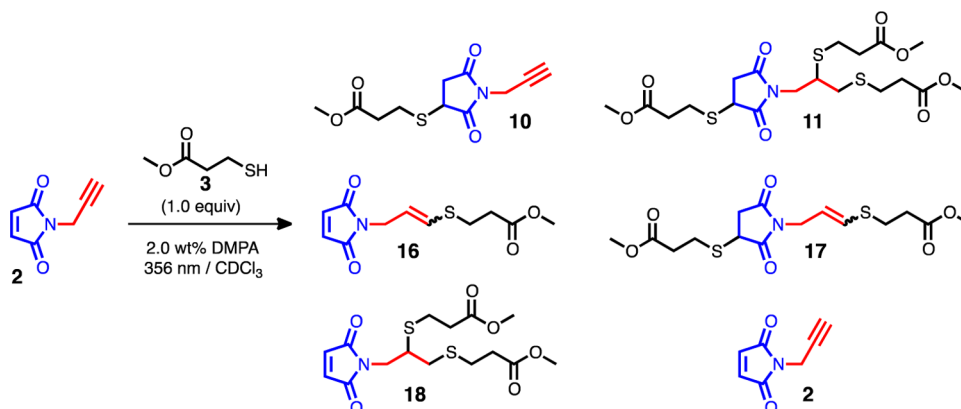
Unselective Thiol–Ene/Thiol–Ene and Thiol–Ene/Thiol–Yne Reactivity. The results outlined above demonstrate complete selectivity in thiol–ene and thiol–yne reactions involving maleimides 1 and 2. Selectivity is achieved when Et₃N-initiated thiol–Michael addition to the maleimide alkene is carried out first, followed thereafter by radical-mediated addition to the allyl or propargyl functionalities. Recent research has also demonstrated^{16b} selectivity in base and nucleophile-initiated thiol–Michael reactions in ternary mixtures of hexane thiol, ethyl vinyl sulfone, and hexyl acrylate. To the best of our knowledge, no examples of the selective radical-mediated addition of a thiol to one alkene in the presence of

Scheme 4. Reaction of *N*-Allyl Maleimide **1** with 1.0 Equiv of Thiol **3** under Radical-Mediated Conditions Gives Unselective Addition to Both Maleimide and Allyl π -Bonds^a



^aExperimental yields are averages of two runs.

Scheme 5. Reacting *N*-Propargyl Maleimide **2** with 1.0 Equiv of Thiol **3** under Radical-Mediated Conditions Results in the Unselective, Complex Addition of Thiol to Maleimide and Propargyl π -Bonds^a



^aThe formation of compounds **11**, **16**, and **17** was not observed experimentally; however, they are included in the scheme for completeness.

another alkene (i.e., ternary thiol–ene–ene systems) have been reported. There have been, however, reports^{25,26} of selective radical-mediated addition of a thiol to an alkyne in the presence of an alkene (ternary thiol–yne–ene systems) allowing, for example, the sequential addition of two different thiols to one alkyne.²⁶ The development of protocols for facile, selective, radical-mediated additions of thiols within ternary systems is of significant synthetic utility. Such protocols can enable sequential one-pot syntheses of polyfunctional materials and polymers, new routes to layered thiol–ene dendrimers, and robust means of selective photochemical nanopatterning of surfaces. Given that electron rich alkenes are known^{1a,c–e,17b,c} to react faster under radical-mediated thiol–ene conditions than electron poor alkenes we sought to investigate whether selectivity would be preserved if the order of reactivity were reversed, i.e. if radical-mediated thiol–ene addition were carried out first followed by thiol–Michael addition.

N-Allyl maleimide **1** was reacted with 1.0 equiv of **3** under radical-mediated conditions (2 wt % DMPA, CHCl₃, 365 nm, Scheme 4). In contrast with the complete selectivity observed when thiol–Michael conditions are used, radical-mediated conditions give a mixture of products **1**, **4**, **5**, and **15** arising from the following: (i) recovered **1**, (ii) addition of **3** to the maleimide double bond of **1** only, (iii) addition of **3** to both maleimide and allyl double bonds of **1**, and (iv) addition of **3** to the allyl double bond of **1** only, respectively. Chromatographic separation of the resulting product mixture revealed that thioether products **4**, **5**, and **15** were formed in approximately 48%, 23%, and 4% yield, respectively, along with 25% recovered starting material (yields are averages of two runs, see the

Supporting Information). It is clear from these results that the more electron poor maleimide π -bond of **1**, which is known to react slowly with thiols under radical-mediated thiol–ene conditions, is consumed to a greater extent than the more electron rich allyl π -bond, which typically undergoes rapid¹⁷ radical-mediated thiol–ene reactions. This observation indicates that kinetics of individual thiol–ene reactions in isolation cannot fully explain the reactivity of a compound containing two different alkenes (e.g., **1**) with only one molar equivalent²⁷ of thiol **3**. Differences in overall thiol–ene click kinetics are known^{16,17} to be governed by the underlying kinetics of individual propagation and chain-transfer steps as well as the stability of the carbon-centered radical intermediate formed following propagation. As a result, ternary thiol–ene reactions^{17c} employing two or more different alkenes often give complex mixtures of products.

The situation becomes even more complex when *N*-propargyl maleimide **2** is allowed to react with 1.0 equiv of thiol **3** under radical-mediated conditions. The presence of three reactive π -bonds in **2** opens the prospect of forming up to five different mono-, di-, or triaddition products. Experimentally, reacting 1.0 equiv of **3** with **2** (2 wt % DMPA, CHCl₃, 365 nm, Scheme 5) does result in a mixture of addition products. Despite considerable effort, attempts to cleanly isolate individual products **10**, **11**, **16**, **17**, and/or **18** from within this complex mixture via column chromatography proved unsuccessful. The crude ¹H NMR spectrum of the ternary thiol–ene/yne reaction between **2** and **3** (Figure S2) indicates a greater amount of the maleimide alkene is consumed than the propargyl alkyne. Furthermore, no proton signals correspond-

ing to a vinyl sulfide could be observed, ruling out the formation of addition products **16** or **17**. Experimental investigations of thiol-yne click chemistry have shown²⁸ that the second addition of thiol is faster than the first, supportive of the fact that vinyl sulfides **16** and **17** are unlikely to be found as they would quickly lead to products **18** or **11**. It could not be determined, chromatographically or by ¹H NMR spectroscopy, whether any triaddition product **11** is formed though its formation is considered unlikely given the 1:1 stoichiometry of starting components **2** and **3**.

In order to more fully understand the complex mixtures of products obtained as shown in Schemes 4 and 5, and the fact that product ratios are not in line with what would be expected given known kinetics of thiol-ene and thiol-yne reactions in isolation, we undertook a computational investigation of the energetics and kinetics of radical-mediated reactions between methyl mercaptan and *N*-substituted maleimides **1** and **2**. Thiol-Michael addition of methyl mercaptan to maleimides **1** and **2** under base-initiated conditions was also investigated to better understand their absolute selectivity. A detailed understanding of the underlying energetics and kinetics of such ternary thiol-ene and thiol-yne reactions will aid significantly in the development of selective, radical-mediated thiol-ene reactions within ternary systems.

■ COMPUTATIONAL INVESTIGATIONS

Compound CBS-QB3 methods²⁹ were used to calculate the relative energetics of base-catalyzed and radical-mediated thiol-ene reactions involving *N*-substituted maleimides **1** and **2**. Previous computational modeling of the radical-mediated¹⁸ and base-initiated³⁰ addition of thiols to alkenes have shown CBS-QB3 to provide energetic and kinetic data that are in good agreement with experimental data. Methyl mercaptan (CH₃SH), methane thiolate (CH₃S⁻), and methyl thiyl radical (CH₃S[•]) were used as model systems for a generic thiol, thiolate anion, and thiyl radical, respectively. The full structures of *N*-allyl maleimide (**1**) and *N*-propargyl maleimide (**2**) were used so that the energetics of propagation and chain transfer steps involving the maleimide, allyl, and propargyl π -bonds could be compared directly. Initiation steps that provide entry into thiol-ene catalytic cycles for both anionic or radical-mediated thiol-ene reactions were not modeled explicitly as initiation kinetics vary with initiator and conditions.^{2c} Instead computational studies focused primarily on determining the energetics and kinetics of each thiol-ene and thiol-yne catalytic cycle. Gas phase CBS-QB3 values were solvent corrected at the B3LYP/6-311G(2d,d,p) level by calculating solvation enthalpies ($\Delta H^\circ_{\text{solv}}$) and free energies ($\Delta G^\circ_{\text{solv}}$) for each structure in a PCM solvent model³¹ for chloroform. All energetics reported and discussed in the subsequent sections are solvent-corrected CBS-QB3 values.

Modeling of Thiol-Michael Additions to **1 and **2**.** Plotted in Figure 3 is a relative free energy diagram of stationary points along the reaction pathways for methane thiolate addition to the maleimide π -bond (left, blue) and allyl π -bond (right, red) of *N*-allyl maleimide (**1**). Also shown in Figure 3 are computed reaction and transition state enthalpies and free energies of individual propagation and chain transfer steps along each pathway. Reaction rates for forward and reverse propagation (k_p , k_{-p}) as well as forward and reverse chain transfer (k_{CT} , $k_{-\text{CT}}$) were calculated using conventional activated complex theory.³²

As can be seen in Figure 3 the addition of methane thiolate to the maleimide π -bond of **1** (i.e., propagation) is found to be a low energy process with a transition state free energy of $\Delta G^\ddagger_p = 7.4$ kcal/mol. The addition is exergonic by $\Delta G^\circ_p = -0.4$ kcal/mol and results in a stabilized enolate anion intermediate. Deprotonation of another equivalent of methyl mercaptan by this enolate intermediate (i.e., chain transfer) has a computed free energy barrier of $\Delta G^\ddagger_{\text{CT}} = 6.2$ kcal/mol relative to the enolate intermediate, leading to the thiol-Michael product. Computed energetics and rate constants for

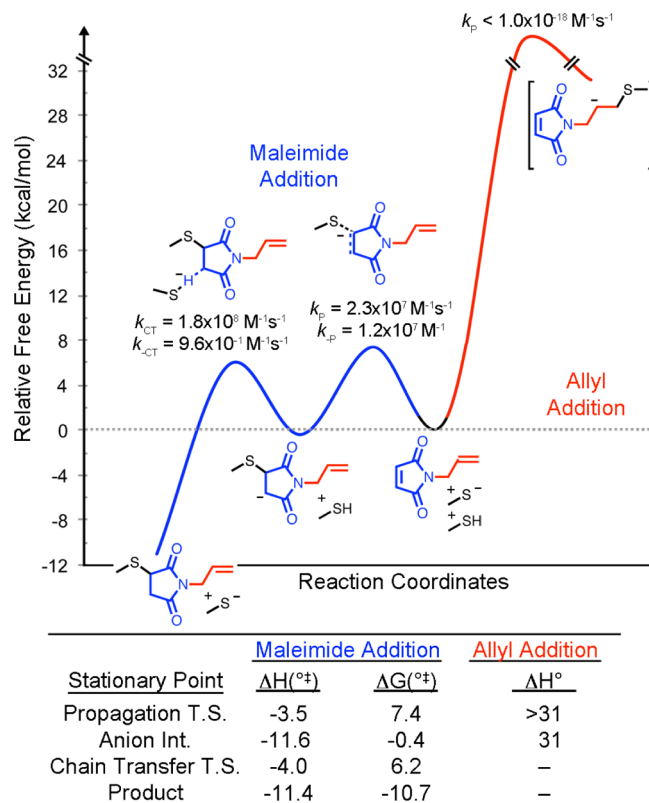


Figure 3. Calculated relative free energy diagram for thiol-Michael addition of methane thiolate to the maleimide (blue pathway) and allyl (red pathway) π -bonds of *N*-allyl maleimide **1**. Reaction and transition state enthalpies and free energies for propagation and chain transfer steps are given in kcal/mol. The free energy barrier for thiolate addition to the allyl π -bond is an estimate, see ref 33.

propagation and chain transfer steps along the maleimide addition pathway suggest that the propagation step is rate limiting ($k_p = 2.3 \times 10^7 \text{ M}^{-1} \text{ s}^{-1}$ vs $k_{\text{CT}} = 1.8 \times 10^8 \text{ M}^{-1} \text{ s}^{-1}$). The computationally predicted rate of $k_p = 2.3 \times 10^7 \text{ M}^{-1} \text{ s}^{-1}$ for the rate determining step of thiolate addition to the maleimide π -bond is in general agreement with experimental studies^{9a} that show the rate to be at least $1 \times 10^7 \text{ M}^{-1} \text{ s}^{-1}$. An alternative reaction pathway involving methane thiolate addition to the allyl π -bond of **1** could not be found despite extensive exploration of the potential energy surface. All attempts to locate a stable carbanion intermediate arising from attack of thiolate anion CH₃S⁻ on the allyl moiety of **1** failed resulting in either (i) rupture of the C_{allyl}-S bond to give starting structures **1** and CH₃S⁻ or (ii) rupture of the *N*-allyl bond of **1** to give allyl(methyl)sulfane and a maleimide anion. Plotted in Figure 3 is an estimate³³ of 31 kcal/mol for the energy of the carbanion intermediate resulting from attack of the allyl moiety of **1** by thiolate anion CH₃S⁻, indicating that the transition state for attack would require $\Delta H^\ddagger_p > 31$ kcal/mol. The greater than 24 kcal/mol difference between thiolate attack of the maleimide π -bond and the allyl π -bond of **1**, and the instability of the resulting anion intermediate, agree with the experimental observation of complete selectivity in Et₃N-initiated thiol-Michael reactions involving *N*-allyl maleimide (**1**). Addition of a thiolate anion to the allyl π -bond of **1** is neither energetically favorable nor kinetically competitive with thiolate addition to the maleimide π -bond.

Figure 4 plots the analogous potential energy surfaces, energetics, and computed rate constants for thiol-Michael addition of methyl mercaptan to *N*-propargyl maleimide **2**. Thiolate addition to the maleimide π -bond is again observed to have a low free energy barrier ($\Delta G^\ddagger_p = 5.7$ kcal/mol), leading to a stabilized enolate intermediate ($\Delta G^\circ_p = -1.8$ kcal/mol). Calculated propagation and chain transfer rates are, within error, identical ($k_p = 4.3 \times 10^8 \text{ M}^{-1} \text{ s}^{-1}$, $k_{\text{CT}} = 2.7 \times 10^8 \text{ M}^{-1} \text{ s}^{-1}$). The most significant difference between propargyl and

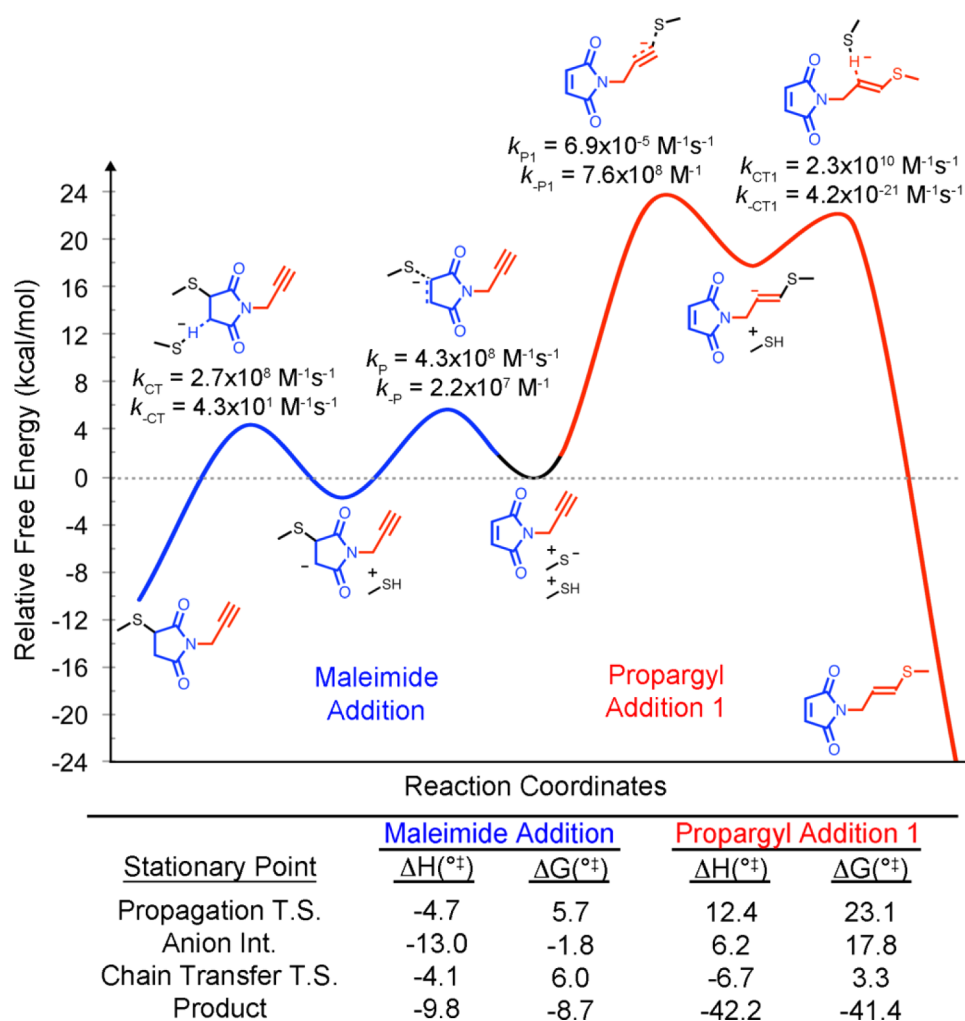


Figure 4. Calculated relative free energy diagram for thiol-Michael addition of methanethiolate to the maleimide (blue pathway) and propargyl (red pathway) π -bonds of *N*-propargyl maleimide **2**. Reaction and transition state enthalpies and free energies for propagation and chain transfer steps are given in kcal/mol. Only one addition of thiol to the propargyl triple bond is favorable.

allyl substituents of functionalized maleimides **1** and **2** is observed in their reactivity toward a thiolate anion CH_3S^- : while neither a propagation transition state nor stable anionic intermediate could be found for thiolate attack of the allyl moiety of **1**, both can be found for thiolate attack of the propargyl moiety of **2** (Figure 4, propargyl addition). Addition of thiolate anion CH_3S^- to the propargyl moiety of **2** is predicted to require $\Delta G_p^\ddagger = 23.1$ kcal/mol. This addition of an electron rich thiolate to an electron rich alkyne to give a vinyl anion is endergonic by $\Delta G_p^\circ = 17.8$ kcal/mol. Chain transfer between this high-energy vinyl anion intermediate and methyl mercaptan is notably more facile, requiring $\Delta G_{CT}^\ddagger = 3.3$ kcal/mol and resulting in a vinyl(methyl)sulfane monoaddition product. A second propagation step corresponding to addition of another equivalent of CH_3S^- to this alkene intermediate could not be found despite extensive searching.³⁴ It is again evident that nucleophilic addition of a thiolate anion to an electron rich alkene is unfavorable, as is supported experimentally. While computational results predict that a first thiolate addition to the propargyl moiety of **2** is possible, it is considerably less favorable than thiolate addition to the maleimide alkene of **2** ($\Delta\Delta G_p^\ddagger = 17.4$ kcal/mol) and leads to a relatively high-energy vinyl anion. These results agree well with the selectivity observed experimentally in Et_3N -initiated reactions shown in Scheme 4.

Modeling of Radical-Mediated Thiol Additions to **1** and **2**.

The relative energetics of radical-mediated thiol additions to maleimides **1** and **2** are of particular interest given the unexpected ratios of products obtained experimentally when each is reacted with 1.0 equiv of methyl-3-mercaptopropionate **3** (Schemes 4 and 5).

Plotted in Figure 5 are the relative free energies of stationary points along the reaction pathways for radical-mediated thiol-ene addition to the maleimide π -bond (left, blue) and allyl π -bond (right, red) of **1**. In contrast to the significant difference in propagation step free energy barriers of methanethiolate addition to **1**, the energetics of addition of methyl thiyl radical to either alkene of **1** are, within error, identical: $\Delta G_p^\ddagger = 10.2$ kcal/mol for addition to the maleimide alkene and $\Delta G_p^\ddagger = 10.0$ kcal/mol for addition to the allyl alkene. By contrast the stability of carbon-centered radical intermediates arising from thiyl attack of the maleimide or allyl π -bonds of **1** differ considerably. Addition of $\text{CH}_3\text{S}^\bullet$ to the maleimide π -bond is predicted to be exergonic by $\Delta G_p^\circ = -2.8$ kcal/mol, while addition to allyl π -bond is endergonic by $\Delta G_p^\circ = 2.0$ kcal/mol. This result agrees with the observation that thiyl additions to electron poor alkenes are generally irreversible, while additions to electron rich alkenes are generally reversible.^{1a,c-e,17} Chain transfer free energy barriers also differ in accordance with the stability of the maleimide or allyl carbon-centered radical intermediate: $\Delta G_{CT}^\ddagger = 12.5$ kcal/mol from the maleimide radical intermediate and 8.9 kcal/mol from the allyl radical intermediate. Overall, thiol-ene reactions with either alkene of **1** are both exergonic.

The similar energetics summarized in Figure 5 imply that the kinetics of thiol addition to the maleimide or allyl moieties of **1** will be competitive. Calculated rates of thiyl addition to either π -bond (k_p) are predicted to be identical within error: $1.9 \times 10^5 \text{ M}^{-1} \text{ s}^{-1}$ for thiyl addition to the maleimide alkene and $2.9 \times 10^5 \text{ M}^{-1} \text{ s}^{-1}$ for thiyl addition to the allyl alkene. Chain transfer rates from the resulting

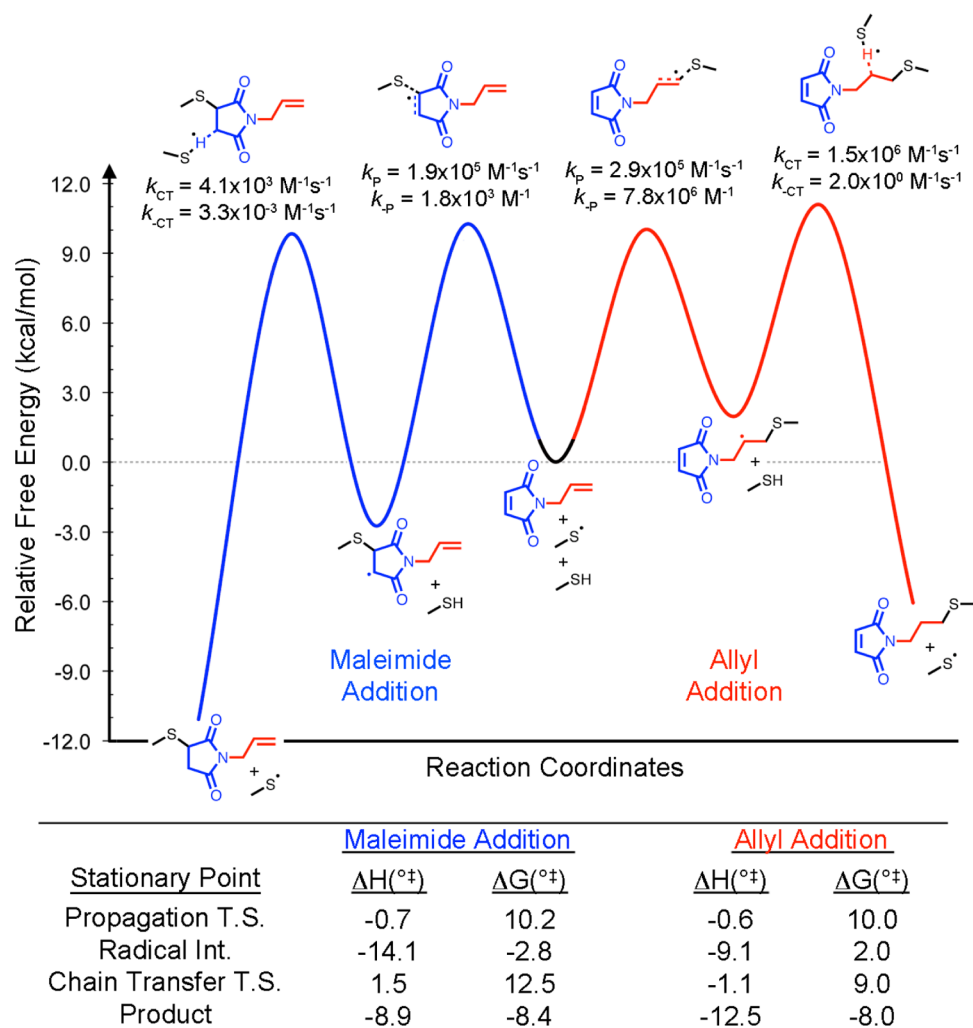
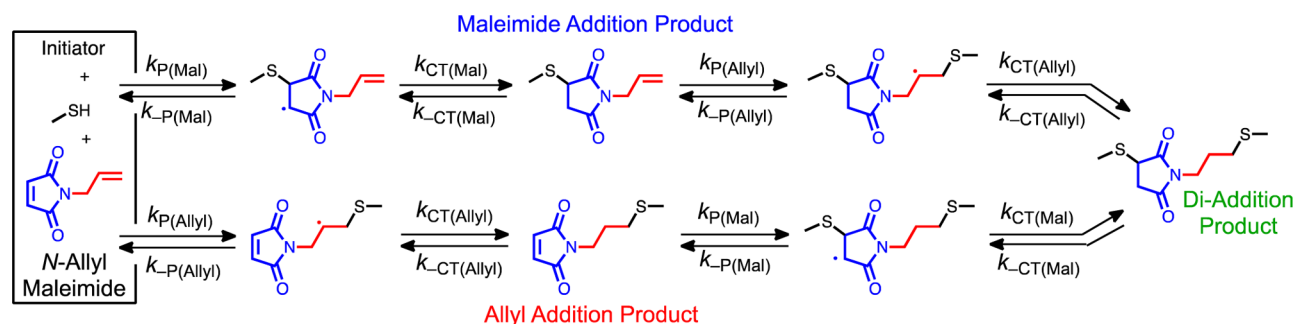


Figure 5. Calculated relative free energy diagram for radical-mediated thiol–ene reactions between methyl mercaptan and the maleimide (blue pathway) and allyl (red pathway) π -bonds of *N*-allyl maleimide **1**. Reaction and transition state enthalpies and free energies for propagation and chain transfer steps are given in kcal/mol.

Scheme 6. Overall Kinetic Scheme Used To Model the Reaction of *N*-Allyl Maleimide with 1.0 Equiv of Methyl Mercaptan^a



^aAll propagation (k_p , k_{-p}) and chain transfer (k_{CT} , k_{-CT}) processes for thiol–ene additions to the maleimide (Mal) and allyl (Allyl) π -bonds were considered to be reversible and in competition with each other. Rate constants for individual steps are those given in Figure 5.

maleimide and allyl radical intermediates are predicted to be $k_{CT} = 4.3 \times 10^3$ and $1.5 \times 10^6 \text{ M}^{-1} \text{ s}^{-1}$, respectively. The chain transfer step is therefore predicted to be rate limiting along the maleimide pathway while propagation is rate limiting along the allyl pathway. Rate constants for reverse propagation (i.e., β -scission) were also calculated and again reveal the notable difference in stability between the maleimide radical intermediate and the allyl radical intermediate. The propagation step involving thiyl addition to the maleimide alkene is largely irreversible with a reverse propagation rate ($k_{-p} = 1.8 \times 10^3$

M^{-1}) that is roughly twice as slow as chain transfer. Thiyl addition to the allyl alkene, however, is more reversible with a reverse propagation rate ($k_{-p} = 7.8 \times 10^6 \text{ M}^{-1}$) that is five times faster than chain transfer.

With rate constants k_p and k_{CT} at hand, the overall reaction between *N*-allyl maleimide (**1**) and 1.0 equiv of methyl mercaptan (Scheme 6) was modeled using the program Kintecus.^{35,36} Initial concentrations of **1** and methyl mercaptan were both taken to be 1.0 M, while the initial concentration of a generic initiator was taken to be 1.0 mM. As shown in Scheme 6 all propagation and chain transfer steps for the radical-

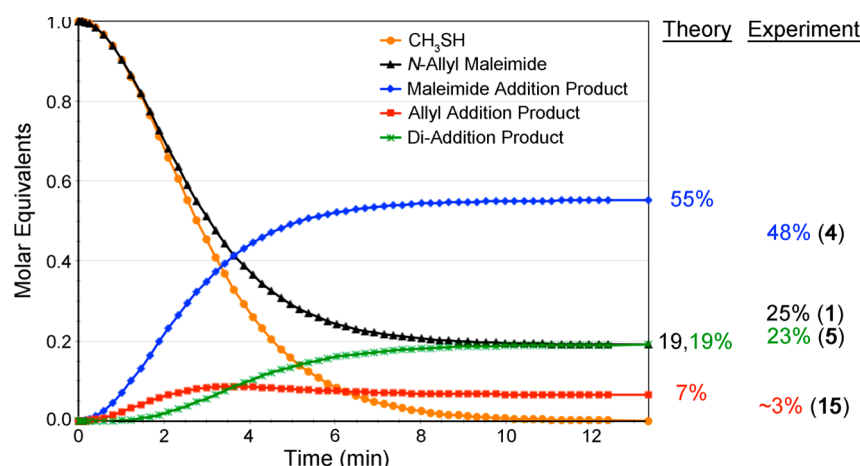


Figure 6. Results of kinetic modeling of the radical-mediated thiol–ene reaction between equimolar equivalents of *N*-allyl maleimide (**1**) with methyl mercaptan. The disappearance of starting materials and appearance of mono- and diaddition products are plotted as a function of time. Experimental yields of analogous products **1**, **4**, **5**, and **15** (Scheme 4) are given for comparison. Modeling reaction parameters: $[1]_0 = [\text{CH}_3\text{SH}]_0 = 1.0 \text{ M}$, $[\text{initiator}]_0 = 1.0 \text{ mM}$, initiation rate $k_i = 1.0 \times 10^{-5} \text{ M}^{-1} \text{ s}^{-1}$.

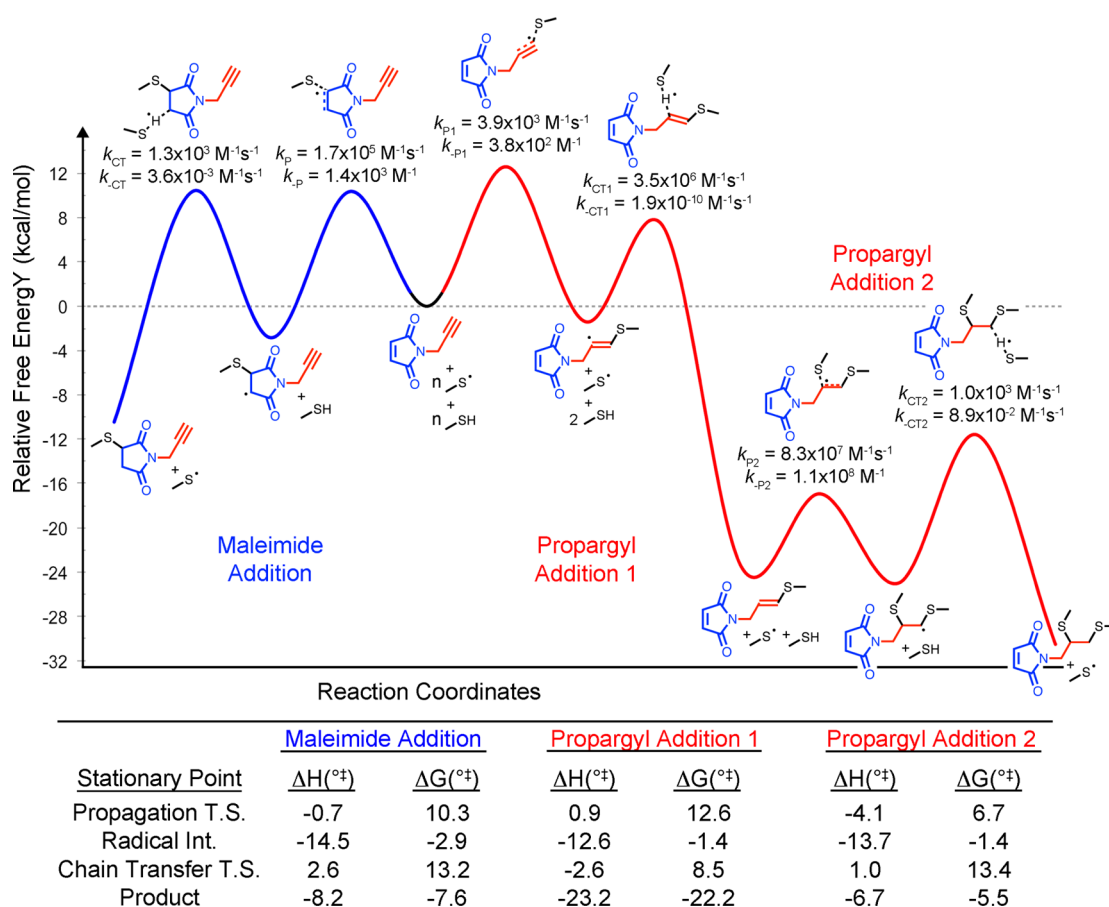


Figure 7. Calculated relative free energy diagram for radical-mediated thiol–ene reactions between methyl mercaptan and the maleimide (blue pathway) and propargyl (red pathway) π -bonds of *N*-propargyl maleimide **2**. Reaction and transition state enthalpies and free energies for propagation and chain transfer steps are given in kcal/mol.

initiated addition of methyl mercaptan to the maleimide and allyl π -bonds of **1** were considered reversible and in competition with each other. In this manner calculated rate constants were used to predict product yields by monitoring the consumption of *N*-allyl maleimide and formation of mono- and diaddition products as a function of time. The results are shown in Figure 6. Computational and kinetic analysis predict that the radical-mediated reaction of equimolar amounts of *N*-allyl maleimide (**1**) and methyl mercaptan will result in a mixture of

monomaleimide addition, monoallyl addition, diaddition, and recovered *N*-allyl maleimide starting material. Furthermore, theoretical analysis suggests thiol addition to the maleimide π -bond is most favored (55%), followed by diaddition and recovered **1** (both 19%), and thiol addition to the allyl π -bond is least favored (7%). These results are in reasonable agreement (Figure 6) with the experimental product mixture obtained upon radical-mediated addition of 1 equiv of thiol **3** to *N*-allyl maleimide **1**. While CBS-QB3 calculations of thiol–

ene kinetics have been shown¹⁸ to be quite accurate, differences between theoretically predicted and experimentally observed product yields may be expected for several reasons, chief among them are the following: (i) methyl mercaptan is used as a model for methyl-3-mercaptopropionate, (ii) chloroform was modeled implicitly rather than explicitly, and (iii) errors inherent in the chromatographic separation of the thiol–ene reaction mixture. Even with these caveats the agreement between experiment and theory is good.

Computational results presented in Figures 5 and 6 are able to help explain the experimental observation that thiol addition to the maleimide π -bond of **1** occurs to a greater extent than addition to the allyl π -bond under radical-mediated conditions. Rates of thiyl radical addition to both alkenes of **1** (propagation step) are predicted to be equal and can be expected to occur to equivalent extents. Chain transfer rates following propagation are more dissimilar, with chain transfer from the allyl-derived radical intermediate being 2 orders of magnitude faster than chain transfer from the maleimide-derived radical intermediate. Reverse propagation of thiyl addition to the allyl π -bond is, however, predicted to be slightly faster than chain transfer, and this reversibility allows more thiyl to equilibrate toward reacting with the maleimide π -bond. The relative stability of the maleimide radical intermediate disfavors reverse propagation such that the majority of thiyl radicals that attack the maleimide π -bond are likely to undergo subsequent chain transfer. While the overall kinetics of thiol–ene addition to the allyl π -bond of **1** are faster, the relative reversibility of thiyl addition to allyl and relative irreversibility of thiyl addition to the maleimide result in greater overall reactivity toward maleimide. Aside from helping explain experimentally observed product distributions these computational results again highlight the complexities of ternary thiol–ene kinetics.

The computed energetics of radical-mediated thiyl addition to the maleimide and propargyl π -bonds of **2** are displayed in Figure 7, along with relative enthalpies and free energies of each step along each pathway and computed propagation and chain transfer rate constants. The free energy barrier for thiyl addition to the maleimide alkene of **2** is predicted to be 2.3 kcal/mol lower than for thiyl addition to its propargyl moiety ($\Delta G^\ddagger = 10.3$ vs 12.6 kcal/mol). Similarly, the rate constant for addition to the maleimide is predicted to be 2 orders of magnitude faster than addition to the propargyl. Chain transfer is again predicted to be the rate-limiting step along the pathway for thiol–ene addition to the maleimide alkene ($k_p = 1.7 \times 10^5 \text{ M}^{-1} \text{ s}^{-1}$ vs $k_{CT} = 1.3 \times 10^3 \text{ M}^{-1} \text{ s}^{-1}$). Propagation is predicted to be rate limiting for the first addition of a thiol to the propargyl moiety of **2** ($k_{p1} = 3.9 \times 10^3 \text{ M}^{-1} \text{ s}^{-1}$ vs $k_{CT1} = 3.5 \times 10^6 \text{ M}^{-1} \text{ s}^{-1}$), which is consistent with experimental investigations of radical-mediated thiol–yne kinetics. Along the 1,2-diaddition thiol–yne pathway, the addition of a second thiyl radical is predicted to be considerably faster than the first ($k_{p1} = 3.9 \times 10^3 \text{ M}^{-1} \text{ s}^{-1}$ vs $k_{p2} = 8.3 \times 10^7 \text{ M}^{-1} \text{ s}^{-1}$). As was stated earlier, thiyl additions to alkenes are generally faster than thiyl additions to alkynes.^{5c,28} This second propagation step, however, is readily reversible as chain transfer from the resulting radical intermediate is predicted to be notably slower than β -scission ($k_{-p2} = 1.1 \times 10^8 \text{ M}^{-1} \text{ s}^{-1}$ vs $k_{CT2} = 1.0 \times 10^3 \text{ M}^{-1} \text{ s}^{-1}$). Overall, the kinetics of radical-mediated thiol–ene addition to the maleimide alkene of **2** are predicted to be faster than thiol–yne 1,2-diaddition to the propargyl π -bonds of **2**.

Kinetic modeling of the reaction between 1.0 equiv of thiol with *N*-propargyl maleimide was carried out using calculated reaction rates shown in Figure 7. The major product predicted theoretically corresponds to the single addition of a thiol to the maleimide π -bond of **2**, which is an analogue of compound **10** (Scheme 5). This compound is predicted to account for 64% of the product mixture. Computations predict recovered *N*-propargyl maleimide (**2**) and the 1,2-diaddition of methyl mercaptan to the propargyl moiety, an analogue of **18**, would each account for 16% of the product mixture. The remaining 4% of the product mixture is predicted to arise from the monoaddition of thiol to the propargyl moiety of **2**, giving a vinyl sulfide analogous to compound **16**. While we were unable to cleanly separate the components of the complex mixture outlined in Scheme 5, there are two notable similarities between computationally predicted and experimentally observed results. For one, computationally

predicted product yields predict that ¹H NMR signals for remaining maleimide alkene at 6.75 ppm and remaining alkyne at 2.21 ppm in the crude product mixture should integrate to a relative ratio of 1.0:1.25 (maleimide:alkyne). This prediction agrees well with the ratio observed experimentally (1.0:1.15, see Figure S2). Second, proton signals corresponding to vinyl sulfide formation could not be observed by ¹H NMR spectroscopy. While computations predict an analogue of vinyl sulfide **16** will form, the vinyl sulfide is predicted to account for only 4% of the product mixture. Experimental and computational results are therefore in reasonable agreement taking into account computational error, experimental error, and NMR detection limits. Lastly, computations predict essentially all vinyl sulfide formed will undergo a subsequent second thiol–ene addition to give a 1,2-diaddition product, which is in line with experimental kinetic studies of thiol–yne click chemistry involving terminal alkynes.²⁸

The greater difference in free energy barriers for addition of a thiyl radical to the maleimide and propargyl π -bonds leads to decreased competition and greater overall selectivity for maleimide addition than is observed with *N*-allyl maleimide **1**. The computed difference of in propagation step free energy barriers ($\Delta\Delta G^\ddagger_p = 2.3$ kcal/mol), however, is not great enough to allow the complete selectivity that is observed in thiolate additions to substituted maleimides **1** and **2**. Overall, computational results support what has been observed experimentally: that radical-mediate thiol additions to maleimides **1** or **2** are not selective. Furthermore, computational results provide a greater understanding of the nonselective nature of radical-mediated thiol–ene and thiol–yne reactions shown in Schemes 4 and 5 by revealing the underlying influence of individual propagation and chain transfer rates on experimentally observed product ratios.

An important outcome of these combined experimental and computational studies is that they provide a theoretical framework for the design of selective radical-mediated thiol–ene and/or thiol–yne reactions. Selectivity in a ternary thiol–ene system would require two alkenes whose reactivities toward thiyl radicals fall within distinct sets of parameters. For example, the propagation step of one alkene, “alkene A”, should be fast (low relative ΔG^\ddagger_p), favorable ($\Delta G^\circ < 0$), and, ideally, rate limiting ($k_p < k_{CT}$). It would then be advantageous for the propagation step of the other alkene, “alkene B”, to be slow (high relative ΔG^\ddagger_p), reversible ($\Delta G^\circ > 0$), and nonrate limiting ($k_p > k_{CT}$). In such a scenario thiyl radicals would be kinetically favored to attack alkene A, forming a relatively stable carbon-centered radical intermediate that would quickly undergo chain transfer to give product A. Should any thiyl radical attack alkene B it would generate a less stable carbon-centered radical intermediate that is more favored to undergo β -scission than chain transfer and therefore unlikely to form product B. Upon complete radical-mediated thiol addition to alkene A, a second thiol could then be promoted to react, albeit slowly, with alkene B. Finding two alkenes that fit these criteria is not trivial, particularly because alkenes that have low propagation barriers and form stable carbon-centered radical intermediates (e.g., butadiene and acrylonitrile) almost universally have high barriers to chain transfer. On the other hand, most alkenes for which propagation is reversible (e.g., vinyl and allyl ethers) also demonstrate fast overall kinetics. It is likely, however, that judicious tuning of electronic and structural properties will enable a suitable pair(s) of alkenes that fit the above criteria to be found. As the current study shows, knowledge of the kinetics of individual thiol–ene reactions in isolation does not provide sufficient information regarding their reactivity in ternary systems; a more complete understanding of individual propagation and chain transfer kinetics is necessary. Further synthesis aided by computational design and mechanistic analysis as described herein may pave the way toward the successful realization of selective, orthogonal radical-mediated thiol–ene click reactions in ternary systems.

CONCLUSIONS

N-Allyl maleimide (**1**) and *N*-propargyl maleimide (**2**) provide facile means of achieving selective Et₃N-initiated thiol–Michael addition to their maleimide alkene followed by radical-mediated thiol–ene/yne addition to their allyl or propargyl functions,

respectively. Selectivity is lost when radical-mediated thiol–ene/yne reactions are carried out first, as the reaction of either 1 or 2 with 1.0 equiv of thiol results in a complex mixture of addition products. CBS-QB3 computational studies reveal that significant differences in the energetics of thiolate (CH_3S^-) addition to the maleimide versus allyl or propargyl π -bonds of 1 and 2 ($\Delta\Delta G^\ddagger > 17$ kcal/mol) underlie their absolute selectivity in thiol–Michael reactions. The energetics of thiyl ($\text{CH}_3\text{S}^\bullet$) addition to the maleimide, allyl, or propargyl π -bonds of 1 or 2 are computationally predicted to be much more similar ($\Delta\Delta G^\ddagger < 2.3$ kcal/mol) and, therefore, competitive. Knowledge of the energetics and kinetics of individual propagation and chain-transfer steps significantly aids in understanding the reactivity of 1 and 2 in radical-mediated thiol–ene/yne reactions. CBS-QB3-based kinetic modeling of competitive thiol–ene/yne reactions involving 1 and 2 predict product distributions that agree well with those observed experimentally, highlighting the utility of combined computational/experimental approaches to understanding ternary thiol–ene/yne reactions. The results have implications in the design and understanding of selective thiol–ene and thiol–yne reactions, most notably within ternary and more complex systems. The maleimide functionalities of 1 and 2 are particularly advantageous given the long established use of maleimides in both bioconjugate chemistry and macromolecular synthesis. We are currently exploring the use of *N*-substituted maleimides 1 and 2 as synthons in the synthesis of dendrimers via selective, sequential thiol–ene/yne chemistry.

EXPERIMENTAL SECTION

General Procedure for Et_3N -Catalyzed Thiol–Michael Reactions. Into a small round-bottom flask was added 1.0 equiv of *N*-allyl maleimide (1)¹⁹ or *N*-propargyl maleimide (2)¹⁹ in chloroform (0.5 M). To the solution was added 1.1 equiv of either methyl-3-mercaptopropionate (3) or β -mercaptoethanol (6) and 0.01 equiv Et_3N . The reaction mixtures were allowed to stir for 5 min, after which volatiles were removed by rotary evaporation followed by further drying under high vacuum ($\sim 10^{-2}$ Torr) giving thiol–Michael addition products in quantitative isolated yields. See the Supporting Information for all ^1H NMR spectra along with full proton assignments.

4: Reaction Scale. 1 (62 mg, 0.45 mmol), yield: 115 mg (99%). The product was isolated as a clear viscous oil. ESI-ACPI (m/z) [$\text{M} + \text{H}$]⁺ Calculated for $\text{C}_{11}\text{H}_{16}\text{NO}_4\text{S}$, 258.0806; found 258.0800. ^1H NMR (CDCl_3 , 300 MHz): δ 5.78 (ddt, 1H, $J = 16.2, 9.6, 5.7$ Hz), 5.23 (d, 1H, $J = 16.2$ Hz), 5.19 (d, 1H, $J = 9.6$ Hz), 4.11 (d, 2H, $J = 5.7$ Hz), 3.79 (dd, 1H, $J = 9.3, 3.6$ Hz), 3.71 (s, 3H), 3.25–3.16 (m, 1H), 3.15 (dd, 1H, $J = 18.6, 9.3$ Hz), 3.07–2.97 (m, 1H), 2.72 (t, 2H, $J = 6.9$ Hz), 2.51 (dd, 1H, $J = 18.6, 3.6$ Hz). ^{13}C NMR (75 MHz, CDCl_3): δ 176.3, 174.2, 172.2, 150.3, 118.7, 52.2, 41.2, 39.2, 36.0, 34.4, 27.1 ppm.

8: Reaction Scale. 1 (57 mg, 0.42 mmol), yield 90 mg (99%). The product was isolated as a clear viscous oil. ESI-ACPI (m/z) [$\text{M} + \text{H}$]⁺ Calculated for $\text{C}_9\text{H}_{14}\text{NO}_3\text{S}$, 216.0700; found 216.0699. ^1H NMR (CDCl_3 , 300 MHz): δ 5.78 (ddt, 1H, $J = 14.1, 7.5, 4.2$), 5.24 (dd, 1H, $J = 14.1, 9.0$ Hz), 5.20 (dd, 1H, $J = 9.0, 7.5$ Hz), 4.11 (d, 2H, $J = 4.2$ Hz), 3.88–3.85 (m, 3H), 3.23–3.11 (m, 2H), 2.93–2.86 (m, 1H), 2.82 (br, 1H), 2.56 (dd, 1H, $J = 14.1, 3.0$ Hz). ^{13}C NMR (75 MHz, CDCl_3): δ 177.5, 174.2, 118.9, 72.1, 62.0, 41.4, 39.7, 36.6, 35.9 ppm.

10: Reaction Scale. 2 (75 mg, 0.56 mmol), yield 141 mg (99%). The product was isolated as a clear viscous oil. ESI-ACPI (m/z) [$\text{M} + \text{H}$]⁺ Calculated for $\text{C}_{11}\text{H}_{14}\text{NO}_4\text{S}$, 256.0638, found 256.0644. ^1H NMR (CDCl_3 , 300 MHz): δ 4.27 (d, 2H, $J = 2.7$ Hz), 3.83 (dd, 1H, $J = 36.1, 9.0$ Hz), 3.71 (s, 3H), 3.23 (dt, 1H, $J = 6.9$ Hz), 3.18 (dd, 1H, $J = 18.9, 9.0$ Hz), 3.03 (dt, 1H, $J = 6.9$ Hz), 2.73 (t, 2H, $J = 6.9$ Hz), 2.53 (dd, 1H, $J = 18.9, 3.9$ Hz), 2.21 (t, 1H, $J = 2.7$ Hz). ^{13}C NMR (75

MHz, CDCl_3): δ 175.4, 173.3, 173.2, 72.0, 52.2, 39.3, 36.1, 34.4, 28.3, 27.1 ppm.

13: Reaction Scale. 2 (105 mg, 0.78 mmol), yield 164 mg (99%). The product was isolated as a clear viscous oil. ESI-ACPI (m/z) [$\text{M} + \text{H}$]⁺ Calculated for $\text{C}_9\text{H}_{12}\text{NO}_3\text{S}$, 214.0532, found 214.0532. ^1H NMR (CDCl_3 , 300 MHz): δ 4.29 (d, 2H, $J = 2.7$ Hz), 3.93–3.88 (m, 3H), 3.21 (dd, 1H, $J = 18.6, 9.0$ Hz), 3.20–3.11 (m, 1H), 2.94–2.86 (m, 1H), 2.60 (dd, 1H, $J = 18.6, 4.2$ Hz), 2.22 (t, 1H, $J = 2.7$ Hz). ^{13}C NMR (75 MHz, CDCl_3): δ 176.5, 173.5, 76.4, 72.4, 62.0, 39.7, 36.6, 35.6, 28.4 ppm.

General Procedure for Radical-Mediated Thiol–Ene/Yne Reactions. 1.0 equiv of thiol–Michael product (4, 8, 10, or 13) was added to a small screw cap glass vial, and the compound was taken up in chloroform (0.5 M). To the solution was added 1.2 equiv (for thiol–ene reactions) or 2.4 equiv (for thiol–yne reactions) of either methyl-3-mercaptopropionate (3) or β -mercaptoethanol (6). The mixtures were stirred until homogeneous, and then 2.0 wt % DMPA was added from a 10 mM freshly prepared stock solution in chloroform. A stream of N_2 gas was passed briefly over the vials, after which they were capped, placed under a UV lamp, and irradiated at 365 nm for 1–3 h to ensure complete consumption of allyl or propargyl moieties. The resulting residues were transferred to round-bottom flasks, concentrated under reduced pressure, dried under high vacuum ($\sim 10^{-2}$ Torr), and passed through a short pad of SiO_2 (eluting with 1:2 hexanes/ethyl acetate) to give pure thiol–ene and thiol–yne products in 96–98% isolated yields.

5: Reaction Scale. 4 (52 mg, 0.20 mmol), yield 75 mg (98%). The product was isolated as a clear viscous oil. ESI-ACPI (m/z) [$\text{M} + \text{H}$]⁺ Calculated for $\text{C}_{15}\text{H}_{24}\text{NO}_6\text{S}_2$, 378.1051; found 378.1053. ^1H NMR (CDCl_3 , 300 MHz): δ 3.78 (dd, 1H, $J = 9.0, 3.6$ Hz), 3.71 (s, 3H), 3.69 (s, 3H), 3.614 (t, 2H, $J = 6.9$ Hz), 3.1 (m, 3H), 2.77 (t, 2H, $J = 6.6$ Hz), 2.72 (t, 2H, $J = 6.9$ Hz), 2.55 (m, 5H), 1.87 (q, 2H, $J = 6.9$ Hz), ppm. ^{13}C NMR (75 MHz, CDCl_3): δ 176.8, 174.7, 172.5, 172.2, 52.2, 52.1, 39.2, 38.4, 36.0, 34.1, 34.4, 29.6, 27.4, 27.1, 27.1 ppm.

7: Reaction Scale. 4 (48 mg, 0.19 mmol), yield 60 mg (96%). The product was isolated as a clear viscous oil. ESI-ACPI (m/z) [$\text{M} + \text{H}$]⁺ Calculated for $\text{C}_{13}\text{H}_{22}\text{NO}_5\text{S}_2$, 336.0945; found 336.0948. ^1H NMR (CDCl_3 , 300 MHz): δ 3.78 (dd, 1H, $J = 9.0$ Hz, 3.6 Hz), 3.71 (t, 2H), 3.71 (s, 3H), 3.64 (t, 2H, $J = 6.9$ Hz), 3.07 (m, 3H), 2.723 (t, 2H, $J = 7.2$ Hz), 2.717 (t, 2H, $J = 6.3$ Hz), 2.53 (t, 2H, $J = 6.9$ Hz), 2.93 (dd, 1H, $J = 18.9, 6.6$ Hz), 2.27 (t, 1H, $J = 6.6$ Hz), 1.88 (q, 2H, $J = 6.9$ Hz), ppm. ^{13}C NMR (75 MHz, CDCl_3): δ 176.3, 174.3, 172.3, 150.3, 118.6, 60.5, 52.2, 41.5, 41.2, 39.2, 36.0, 34.4, 27.1 ppm.

9: Reaction Scale. 8 (35 mg, 0.16 mmol), yield 52 mg (96%). The product was isolated as a clear viscous oil. ESI-ACPI (m/z) [$\text{M} + \text{H}$]⁺ Calculated for $\text{C}_{13}\text{H}_{22}\text{NO}_5\text{S}_2$, 336.0945, found 336.0949. ^1H NMR (CDCl_3 , 300 MHz): δ 3.86 (t, 1H, $J = 8.1$ Hz), 3.83 (dd, 1H, 3.6, 0.9 Hz), 3.68 (s, 3H), 3.60 (t, 2H, $J = 7.2$ Hz), 3.20–3.07 (m, 2H), 2.92–2.83 (m, 1H), 2.75 (t, 2H, $J = 7.2$ Hz), 2.58 (t, 2H, $J = 7.2$ Hz), 2.56–2.49 (m, 3H), 1.86 (p, 2H, $J = 7.2$ Hz), ppm. ^{13}C NMR (75 MHz, CDCl_3): δ 177.9, 174.7, 172.6, 150.3, 62.1, 52.1, 39.7, 38.5, 36.6, 34.8, 29.6, 27.1 ppm.

11: Reaction Scale. 10 (81 mg, 0.32 mmol), yield 152 mg (97%). The product was isolated as a clear viscous oil. ESI-ACPI (m/z) [$\text{M} + \text{H}$]⁺ Calculated for $\text{C}_{19}\text{H}_{30}\text{NO}_6\text{S}_3$, 496.1128, found 496.1147. ^1H NMR (CDCl_3 , 300 MHz): δ 3.85–3.78 (m, 3H), 3.66 (s, 9H), 3.62–3.58 (m, 1H), 3.22–3.11 (m, 4H), 3.03–2.93 (m, 1H), 2.80 (t, 6H, $J = 7.2$ Hz), 2.69 (t, 2H, $J = 7.2$ Hz), 2.60 (t, 2H, $J = 7.2$ Hz), 2.47 (dd, 1H, $J = 18.9, 3.6$ Hz), ppm. ^{13}C NMR (75 MHz, CDCl_3): δ 176.8, 176.8, 174.8, 172.5, 172.2, 150.3, 74.4, 52.1, 43.4, 42.0, 39.3, 36.5, 36.0, 34.9, 34.7, 34.4, 27.9, 27.1, 25.9 ppm.

12: Reaction Scale. 10 (45 mg, 0.17 mmol), yield 70 mg (96%). The product was isolated as a clear viscous oil. ESI-ACPI (m/z) [$\text{M} + \text{H}$]⁺ Calculated for $\text{C}_{15}\text{H}_{26}\text{NO}_6\text{S}_3$, 412.0917, found 412.0916. ^1H NMR (CDCl_3 , 300 MHz): δ 3.90–3.65 (m, 8H), 3.70 (s, 3H), 3.23–3.12 (m, 4H), 3.08–2.97 (m, 1H), 2.83–2.70 (m, 6H), 2.64 (br, 2H), 2.53 (dd, 1H, $J = 18.9, 3.5$ Hz), ppm. ^{13}C NMR (75 MHz, CDCl_3): δ 176.8, 174.8, 172.2, 52.1, 43.4, 42.0, 39.3, 36.5, 36.0, 34.9, 34.7, 34.4, 27.8, 27.1, 26.0 ppm.

14: Reaction Scale. 11 (93 mg, 0.44 mmol), yield 192 mg (97%). The product was isolated as a clear viscous oil. ESI-ACPI (m/z) [$M + H$]⁺ Calculated for $C_{17}H_{28}NO_5S_3$, 454.1022, found 454.1040. ¹H NMR ($CDCl_3$, 300 MHz): δ 3.86 (ddd, 1H, $J = 9.2, 4.2, 2.1$ Hz), 3.83–3.78 (m, 3H), 3.76 (dd, 1H, $J = 4.2, 2.1$ Hz), 3.63 (s, 3H), 3.62 (s, 3H), 3.57 (dd, 1H, $J = 4.2, 2.1$ Hz), 3.19 (dd, 1H, $J = 9.1, 4.8$ Hz), 3.13 (dd, 2H, $J = 9.2, 2.1$ Hz), 3.08–3.01 (m, 1H), 2.88–2.82 (m, 1H), 2.81–2.72 (m, 4H), 2.66 (ddd, 1H, $J = 13.8, 5.7, 4.8$ Hz), 2.58–2.50 (m, 4H), ppm. ¹³C NMR (75 MHz, $CDCl_3$): δ 177.9, 174.8, 172.5, 172.3, 62.0, 52.1, 43.4, 42.1, 39.8, 36.5, 36.0, 34.9, 34.7, 34.1, 33.3, 27.9, 25.9 ppm.

Computational Details. All calculations were performed with the Gaussian09 suite of programs.³⁷ Prior to geometry optimization to full convergence, potential energy surfaces of all structures were thoroughly explored by scanning all freely rotating dihedral angles at the HF/6-31G* level to locate their approximate global minimum energy conformations. Full geometry optimization, vibrational, and thermal analysis were then performed with the CBS-QB3 compound method.²⁹ Transition states searches were performed by one of two methods: (1) performing relaxed potential energy surface scans of the bond coordinate(s) corresponding to bond breaking/formation or (2) using the QST2 method.³⁸ Transition states were then refined using a Berny optimization with the CBS-QB3 method. Transition states were distinguished as having a single imaginary vibrational frequency corresponding to the vibrational mode connecting reactants and products and were confirmed with IRC calculations. CBS-QB3 optimizations of minima and transition states were performed in the gas phase at 1.0 atm pressure and 298.15 K. Enthalpies and free energies of solvation for each stationary point were calculated as the difference in energy between gas phase and solution phase (chloroform, $\epsilon = 4.7113$) structures optimized at the B3LYP/6-311G(2d,d,p) level.

■ ASSOCIATED CONTENT

● Supporting Information

Full synthetic details, characterization, and spectra, Cartesian coordinates of all stationary points reported in this manuscript and their absolute energies in hartrees, kinetic modeling plots, and the full author list for ref 37. This material is available free of charge via the Internet at <http://pubs.acs.org>.

■ AUTHOR INFORMATION

Corresponding Author

*E-mail: bnorthrop@wesleyan.edu

Notes

The authors declare no competing financial interest.

■ ACKNOWLEDGMENTS

We are grateful to the ACS PRF for financial support through a research grant to B.H.N. and to the Howard Hughes Medical Institute for summer undergraduate research support to R.M.S. We thank Wesleyan University for computer time supported by the NSF under grant number CNS-0619508. We thank the University of California, Riverside Mass Spectrometry facility for mass spectrometric analysis.

■ REFERENCES

- (1) (a) Hoyle, C. E.; Lee, T. Y.; Roper, T. J. *Polym. Sci., Part A: Polym. Chem.* **2004**, *42*, 5301. (b) Dondoni, A. *Angew. Chem., Int. Ed.* **2008**, *47*, 8995. (c) Lowe, A. B. *Polym. Chem.* **2010**, *1*, 17. (d) Hoyle, C. E.; Bowman, C. N. *Angew. Chem., Int. Ed.* **2010**, *49*, 1540. (e) Hoyle, C. E.; Lowe, A. B.; Bowman, C. N. *Chem. Soc. Rev.* **2010**, *39*, 1355. (f) Kade, M. J.; Burke, D. J.; Hawker, C. J. *J. Polym. Sci., Part A: Polym. Chem.* **2010**, *48*, 743.
- (2) See, for example: (a) Justynska, J.; Schlaad, H. *Macromol. Rapid Commun.* **2004**, *25*, 1478. (b) Brummelhuis, N. T.; Diehl, C.; Schlaad,

H. *Macromolecules* **2008**, *41*, 9946. (c) Campos, L. M.; Killops, K. L.; Sakai, R.; Paulusse, J. M. J.; Dameron, D.; Drockenmüller, E.; Messmore, B. W.; Hawker, C. J. *Macromolecules* **2008**, *41*, 7063.

(3) For representative examples of the use of thiol–ene chemistry in the synthesis of biomaterials, see: (a) Wittrock, S.; Becker, T.; Kunz, H. *Angew. Chem., Int. Ed.* **2007**, *46*, 5226. (b) Triola, G.; Brunsvel, L.; Waldmann, H. *J. Org. Chem.* **2008**, *73*, 3646. (c) Jones, M. W.; Mantovani, G.; Ryan, S. M.; Wang, X.; Brayden, D. J.; Haddleton, D. M. *Chem. Commun.* **2009**, 5272. (d) Boyer, C.; Davis, T. P. *Chem. Commun.* **2009**, 6029. (e) Gu, W.; Chen, G.; Stenzel, M. H. *J. Polym. Sci., Part A: Polym. Chem.* **2009**, *47*, 5550. (f) Dondoni, A.; Marra, A. *Chem. Soc. Rev.* **2012**, *41*, 573.

(4) For representative examples of the application of thiol–ene chemistry in materials fabrication, see: (a) Hagberg, E. C.; Malkoch, M.; Ling, Y.; Hawker, C. J.; Carter, K. R. *Nano Lett.* **2007**, *7*, 233. (b) Khire, V. S.; Yi, Y.; Clark, N. A.; Bowman, C. N. *Adv. Mater.* **2008**, *20*, 3308. (c) Campos, L. M.; Meinel, I.; Guino, R. G.; Schierhorn, M.; Gupta, N.; Stucky, G. D.; Hawker, C. J. *Adv. Mater.* **2008**, *20*, 3728.

(5) (a) Lowe, A. B.; Hoyle, C. E.; Bowman, C. N. *J. Mater. Chem.* **2010**, *20*, 4745. (b) Hoogenboom, R. *Angew. Chem., Int. Ed.* **2010**, *49*, 3415. (c) Massi, A.; Nanni, D. *Org. Biomol. Chem.* **2012**, *10*, 3791.

(6) (a) Kold, H. C.; Finn, M. G.; Sharpless, K. B. *Angew. Chem., Int. Ed.* **2001**, *40*, 2004. (b) Mose, J. E.; Moorhouse, A. D. *Chem. Soc. Rev.* **2007**, *36*, 1249.

(7) Barner-Kowollik, C.; Du Prex, F. E.; Espeel, P.; Hawker, C. J.; Junkers, T.; Schlaad, H.; Camp, W. V. *Angew. Chem., Int. Ed.* **2011**, *50*, 60.

(8) While thiol–ene reactions have been classified as a “click” technique for approximately a decade, some recent research has cast doubt as to whether this should be the case, see: Derboven, P.; D’hooge, D. R.; Stamenovic, M. M.; Espeel, P.; Marin, G. B.; Du Prez, F. E.; Reyniers, M.-F. *Macromolecules* **2013**, *46*, 1732.

(9) (a) Chan, J. W.; Hoyle, C. E.; Lowe, A. B.; Bowman, M. *Macromolecules* **2010**, *43*, 6381. (b) Li, G.-Z.; Randev, R. K.; Soeriyadi, A. H.; Rees, G.; Boyer, C.; Tong, Z.; Davis, T. P.; Becer, C. R.; Haddleton, D. M. *Polym. Chem.* **2010**, *1*, 1196. (c) Truong, V. X.; Dove, A. P. *Angew. Chem., Int. Ed.* **2013**, *52*, 4132. (d) Lowe, A. B.; Chan, J. W. *Thiol–Yne Chemistry in Polymer and Materials Science*. In *Functional Polymers and Post-Polymerization Modification: Concepts, Guidelines, and Applications*; Theato, P.; Klok, H.-A., Eds.; Wiley-VCH: Weinheim, Germany, 2013; pp 87–116.

(10) Tolstyka, Z. P.; Kopping, J. T.; Maynard, H. D. *Macromolecules* **2008**, *41*, 599.

(11) Chan, J. W.; Hoyle, C. E.; Lowe, A. B. *J. Am. Chem. Soc.* **2009**, *131*, 5751.

(12) Yu, B.; Chan, J. W.; Hoyle, C. E.; Lowe, A. B. *J. Polym. Sci., Part A: Polym. Chem.* **2009**, *47*, 3544.

(13) Shen, Y.; Ma, Y.; Li, Z. *J. Polym. Sci., Part A: Polym. Chem.* **2013**, *51*, 708.

(14) Nair, D. P.; Cramer, N. B.; Gaipa, J. C.; McBride, M. K.; Matherly, E. M.; McLeod, R. R.; Shandas, R.; Bowman, C. N. *Adv. Funct. Mater.* **2012**, *22*, 1502.

(15) It should be noted that bis-maleimides have been used for sequential thiol–Michael click reactions before; however, sequential reactivity was achieved by using excess bis-maleimide rather than inherently selective thiol–ene reactions, see: Li, M.; De, P.; Gondi, S. R.; Sumerlin, B. S. *J. Polym. Sci., Part A: Polym. Chem.* **2008**, *46*, 5093.

(16) Recent research has found that vinyl sulfones also undergo very rapid thiol–Michael addition reactions, and their kinetics may rival maleimides under some conditions, see: (a) Xi, W.; Kloxin, C. J.; Bowman, C. N. *ACS Macro Lett.* **2012**, *1*, 811. (b) Chatani, S.; Nair, D. P.; Bowman, C. N. *Polym. Chem.* **2013**, *4*, 1048.

(17) For experimental investigations of the influence of alkene functionality on thiol–ene kinetics, see: (a) Cramer, N. B.; Reddy, S. K.; O’Brien, A. K.; Bowman, C. N. *Macromolecules* **2003**, *36*, 7964. (b) Reddy, S. K.; Cramer, N. B.; Bowman, C. N. *Macromolecules* **2006**, *39*, 3673. (c) Reddy, S. K.; Cramer, N. B.; Bowman, C. N. *Macromolecules* **2006**, *39*, 3681.

- (18) For a theoretical investigation of the influence of alkene functionality on thiol–ene kinetics, see: Northrop, B. H.; Coffey, R. N. *J. Am. Chem. Soc.* **2012**, *134*, 13804.
- (19) Clevenger, R. C.; Turnbull, K. D. *Synth. Commun.* **2000**, *30*, 1379.
- (20) We have been able to successfully catalyze the thiol–Michael reaction between **1** and **3** at lower catalyst loading, down to 0.001 equiv of Et₃N, but typically run these reactions at 0.01 equiv Et₃N for greater ease of measurement and transfer.
- (21) Separation of desired products from trace DMPA side products and residual thiol is achieved by passing the crude mixture through a short pad of silica.
- (22) See, for example: (a) Miyadera, T.; Kosower, E. M. *J. Med. Chem.* **1972**, *15*, 534. (b) Ghosh, S. S.; Koa, P. M.; McCue, A. W.; Chappelle, H. L. *Bioconjugate Chem.* **1990**, *1*, 71. (c) Gindy, M. E.; Ji, S.; Hoye, T. R.; Panagiotopoulos, A. Z.; Prud'homme, R. K. *Biomacromolecules* **2008**, *9*, 2705. (d) Yeh, H.-Y.; Yates, M. V.; Mulchandani, A.; Chen, W. *Proc. Natl. Acad. Sci. U.S.A.* **2008**, *105*, 17522. (e) Radu, L. C.; Yang, J.; Kopecek, J. *Macromol. Biosci.* **2009**, *9*, 36.
- (23) (a) Gramlich, P. M. E.; Wirges, C. T.; Manetto, A.; Carell, T. *Angew. Chem., Int. Ed.* **2008**, *47*, 8350. (b) Lallana, E.; Riguera, R.; Fernandez-Megia, E. *Angew. Chem., Int. Ed.* **2011**, *50*, 8794. (c) El-Sagheer, A. H.; Brown, T. *Acc. Chem. Res.* **2012**, *45*, 1258.
- (24) Several methods of copper-free alkyne–azide cycloadditions have also been developed in recent years, see: (a) Baskin, J. M.; Prescher, J. A.; Laughlin, S. T.; Agard, N. J.; Chang, P. V.; Miller, I. A.; Lo, A.; Codelli, J. A.; Bertozzi, C. R. *Proc. Natl. Acad. Sci. U.S.A.* **2007**, *104*, 16793. (b) Jewett, J. C.; Bertozzi, C. R. *Chem. Soc. Rev.* **2010**, *39*, 1272.
- (25) Fairbanks, B. D.; Sims, E. A.; Anseth, K. S.; Bowman, C. N. *Macromolecules* **2010**, *43*, 4113.
- (26) Conte, M. L.; Pacifico, S.; Chambery, A.; Marra, A.; Dondoni, A. *J. Org. Chem.* **2010**, *75*, 4644.
- (27) It should be noted that when *N*-allyl maleimide **1** is allowed to react with 2.2 or more equiv of thiol **3** under the same conditions (CHCl₃, 2 wt % DMPA, 365 nm) complete conversion to diaddition product **5** is observed.
- (28) (a) Fairbanks, B. D.; Scott, T. F.; Kloxin, C. J.; Anseth, K. S.; Bowman, C. N. *Macromolecules* **2009**, *42*, 211.
- (29) (a) Nyden, M. R.; Petersson, G. A. *J. Chem. Phys.* **1981**, *75*, 1843. (b) Petersson, G. A.; Al-Laham, M. A. *J. Chem. Phys.* **1991**, *94*, 6081. (c) Petersson, G. A.; Tensfeldt, T.; Montgomery, J. A. *J. Chem. Phys.* **1991**, *94*, 6091. (d) Montgomery, J. A.; Ochterski, J. W.; Petersson, G. A. *J. Chem. Phys.* **1994**, *101*, 5900.
- (30) Krenske, E. H.; Petter, R. C.; Zhu, Z.; Houk, K. N. *J. Org. Chem.* **2011**, *76*, 5074.
- (31) (a) Miertus, S.; Scrocco, E.; Tomasi, J. *Chem. Phys.* **1981**, *55*, 117. (b) Cossi, M.; Barone, V.; Cammi, R.; Tomasi, J. *Chem. Phys. Lett.* **1996**, *255*, 327.
- (32) McQuarrie, D. A.; Simon, J. D. *Chemical Kinetics I: Rate Laws*. In *Physical Chemistry: A Molecular Approach*; University Science Books: Sausalito, CA, 1997; pp 1165–1169.
- (33) This estimate was obtained by performing a full conformational search of the model anion intermediate while constraining the C_{allyl}–S bond to be 1.80 Å and the N–allyl bond to be 1.45 Å. A single-point CBS-QB3 calculation was then performed on the lowest energy conformation obtained from this restricted conformational search by invoking the keyword iop(1/7=1000000) to ensure convergence by the first cycle. Only the relative enthalpy of this model anion is reported as thermal frequency calculations do not have any meaning for structures that are not true minima or transition states. For additional details regarding how this estimate was obtained see the Supporting Information.
- (34) A procedure analogous to that outlined in ref 33 was used to obtain an estimate for the electronic energy of the anion intermediate obtained from thiolate addition to the π -bond of the vinyl sulfide intermediate.
- (35) Ianni, J. C. *Kintecus*, version 3.82; 2005. www.kintecus.com (accessed Aug 2, 2013).
- (36) For a complete explanation of the kinetic modeling procedure see the Supporting Information.
- (37) Frisch, M. J. et al. *Gaussian 09, Revision A.1*; see the Supporting Information.
- (38) Peng, C.; Ayala, P. Y.; Schlegel, H. B.; Frisch, M. J. *Comput. Chem.* **1996**, *17*, 49.